Paper # 087MK-0012 **Topic: Chemical Kinetics**

Western States Section of the Combustion Institute
California Institute of Technology
March 23-25, 2014.

Thermal Ignition - One-Step Modeling of the Transition from Slow Reactions to Ignition

P. A. Boettcher[*1], *V. L. Thomas*[2], *R. Mével*[3]

[1]*Mechanical Engineering and Mechanics,*
Drexel University, Philadelphia, PA 19104, USA
[2]*Mechanical Engineering,*
Johns Hopkins University, Baltimore, MD 21218
[3]*Graduate Aeronautics Laboratory (GALCIT),*
California Institute of Technology, Pasadena, California 91125, USA

Thermal ignition of flammable gaseous mixtures from a hot surface is a major concern for a wide range of industrial activities. When homogeneous hydrocarbon fuel/oxidizer mixtures are heated in a closed vessel from room temperature to around the autoignition temperature the mixture can undergo either a slow reaction or an ignition if heat is allowed to transfer to the surroundings. Experiments and simulations using detailed chemical mechanism have shown that this behavior is a function of the heating rate, the initial composition, and the initial pressure. The present study aims at developing a one-step reaction model which captures the transition from slow to fast reaction for a wide range of conditions. In particular, the one-step model includes the effects of pressure and changes in initial composition. Such a model could be included in multi-dimensional simulations to investigate the risk of hot surface ignition under complex industrial configurations.

1 Introduction

Thermal ignition of flammable gaseous mixtures from a hot surface is a major concern for a wide range of industrial activities including commercial aviation, nuclear power plants and industrial chemical processes. Minimizing the risk of accidental combustion events through more relevant safety regulations and improved engineering design demands a deep understanding of thermal ignition phenomenon. In a previous study [2] on the autoignition of hexane/air mixtures, we have experimentally demonstrated that a flammable mixture submitted to a range of heating rates can undergoes either a slow reaction or an ignition event. The slow reaction was characterized by a slow consumption of the reactants at essentially constant temperature and pressure, while the ignition was associated with a thermal runaway and significant pressure increase. The mixture is observed to transition to ignition with increasing heating rate, pressure, and equivalence ratio for the limited range of $\phi = 0.7 - 1.4$. This behavior was also investigated computationally using a detailed chemical mechanism [2]. The computational model extends the classical Semenov theory by including a term for the rate at which the mixture is heated [7]. Detailed analyses of the chemical reaction pathways and energy balance have demonstrated than the competition between the chemical energy release rate and heat losses rate in the vicinity of the auto-ignition temperature can induce a composition change so that an initially flammable mixture becomes non-flammable.

Despite the insight provided by the detailed simulations, the large number of chemical species and reactions involved during low-temperature oxidation of hydrocarbon fuels makes the computation too expensive for studying complex industrial configurations through multi-dimensional numerical simulations.

The present study aims at developing a computationally inexpensive one-step chemical model which captures the transition behavior from slow to fast reaction due to changes in heating rate, initial pressure and composition (equivalence ratio) a over wide range of conditions. We first describe the governing equations, then show the results of the simulations and finally discuss the observed behavior.

2 Thermal Ignition Model

We model this thermal ignition process using a thermodynamic and chemical kinetic model. The thermodynamic model is given by the conservation of energy equation for the constant volume and constant mass system,

$$mc_v \frac{dT}{dt} = \dot{Q}_r + \dot{Q}_w \ , \tag{1}$$

where the energy release rate due to chemical reactions, $\dot{Q}_r$, is in competition with the energy transfer rate at the wall, $\dot{Q}_w$. The heat transfer with the wall is expanded from the original Semenov theory to include the initial temperature of the wall, T_w^0, and the rate at which it is heated, α [2, 7]. The heat transfer at the wall is then

$$\dot{Q}_w = Sh\left(T_w^0 + \alpha\, t - T\right) \ . \tag{2}$$

2.1 Energy Release Rate

The energy release rate is found by assuming that the reaction progresses in one irreversible step from reactant, R, to product, P:

$$R \rightarrow P. \tag{3}$$

The rate at which this reaction progresses depends on, T, the temperature and, $[R]$, the molar concentration of reactant [4].

$$\frac{d[P]}{dt} = -\frac{d[R]}{dt} = \dot{\omega} = k(T)[R]^n \tag{4}$$

In equation 4, $\dot{\omega}$ is the molar production rate per unit volume, k is the reaction rate, and n is the effective reaction order. Using the approach from [1], we express the molar concentration using ideal gas law, $pV = n\tilde{R}T$,

$$[i] = \frac{n_i}{V} = \frac{p_i}{\tilde{R}T} = \frac{X_i p}{\tilde{R}T} = \frac{X_i}{W_i}\rho \ , \tag{5}$$

where n_i, p_i, X_i, and W_i are the number of moles, the partial pressure, the mole fraction, and the molecular weight, respectively, of either the reactant, R, or the product, P. The variables p, and ρ

are mixture pressure and density, respectively. The reaction is ultimately be expressed in the form of the reaction progress variable, λ, which is equivalent to the mass fraction of the products, Y_P.

$$Y_P = X_P \frac{W_P}{W} \tag{6}$$

We express Equation 4 in terms of mass fraction using Equations 5 and 6

$$\frac{d[P]}{dt} = \frac{dX_P}{dt}\frac{\rho}{W_P} = \frac{dY_P}{dt}\frac{W}{W_P^2}\rho \,. \tag{7}$$

Solving for dY_P/dt yields

$$\frac{dY_P}{dt} = \frac{W_P^2}{W\rho}k(T)[R]^n \tag{8}$$

$$\frac{dY_P}{dt} = \frac{W_P^2}{W}\frac{1}{\rho}k(T)\left(\frac{X_R}{W_R}\rho\right)^n \,. \tag{9}$$

The rate of progress of the chemical reaction is governed by an Arrhenius rate law [4],

$$k(T) = A\exp\left(-\frac{E_a}{\tilde{R}T}\right) , \tag{10}$$

where A is the pre-exponential, E_a is the activation energy and $\tilde{R}$ is the universal gas constant. Substituting Equation 10 into Equation 9, the evolution of the mass fraction of P becomes

$$\frac{dY_P}{dt} = \frac{W_P^2}{W}\frac{1}{\rho}\left(\frac{X_R}{W_R}\rho\right)^n A\exp\left(-\frac{E_a}{\tilde{R}T}\right) , \tag{11}$$

$$\frac{dY_P}{dt} = \left(A\frac{W_P^2}{W}\frac{X_R^n}{W_R^n}\right)\rho^{n-1}\exp\left(-\frac{E_a}{\tilde{R}T}\right) . \tag{12}$$

We combine the terms in parenthesis in Equation 12 and assign them to the pre-exponential factor Z [1]. In addition, we restate the equation in terms of progress variable, λ, introducing the consumption term, $(1-\lambda)$.

$$\frac{d\lambda}{dt} = Z(1-\lambda)\rho^{n-1}\exp\left(-\frac{E_a}{\tilde{R}T}\right) \tag{13}$$

When $\lambda = 0$ the mass fraction of R is 1; when $\lambda = 1$ the mass fraction of P is 1.

The energy release rate is then

$$\dot{Q}_r = mq_c\frac{d\lambda}{dt} = mq_cZ(1-\lambda)\rho^{n-1}\exp\left(-\frac{E_a}{\tilde{R}T}\right) . \tag{14}$$

where q_c is the chemical energy content per unit mass of R and m is the mass of the gas.

The coupled equations describing this thermal ignition model are

$$\frac{dT}{dt} = \frac{q_c}{c_v}Z(1-\lambda)\rho^{n-1}\exp\left(-\frac{E_a}{\tilde{R}T}\right) + \frac{Sh}{mc_v}\left(T_w^0 + \alpha\, t - T\right) \,, \tag{15}$$

$$\frac{d\lambda}{dt} = Z(1-\lambda)\rho^{n-1}\exp\left(-\frac{E_a}{\tilde{R}T}\right) . \tag{16}$$

2.2 Effect of Initial Pressure

A change in the initial pressure will change the mass contained in the constant volume considered.

$$\frac{dT}{dt} = \frac{q_c}{c_v}\frac{d\lambda}{dt} + \frac{Sh}{mc_v}\left(T_w^0 + \alpha\, t - T\right) \tag{17}$$

The mass, m, can be expressed in terms of the initial pressure and temperature using the ideal gas law, $pV = mRT$.

$$\frac{dT}{dt} = \frac{q_c}{c_v}\frac{d\lambda}{dt} + \frac{Sh}{c_v}\frac{RT^0}{p^0 V}\left(T_w^0 + \alpha\, t - T\right) \tag{18}$$

Increases in the initial pressure decrease the magnitude of the wall heat transfer term. Thus, increasing the pressure should transition the mixture from a slow reaction case to an ignition case. However, when the effective reaction order, n, is greater than 1, the pressure also influences the heat release term, $\dot{Q}_r$, by influencing the rate of reaction progress.

$$\frac{dT}{dt} = \frac{q_c}{c_v} Z(1-\lambda)\left(\frac{p^0}{RT^0}\right)^{n-1} \exp\left(-\frac{E_a}{\tilde{R}T}\right) + \frac{Sh}{c_v}\frac{RT^0}{p^0 V}\left(T_w^0 + \alpha\, t - T\right) \tag{19}$$

$$\frac{d\lambda}{dt} = Z(1-\lambda)\left(\frac{p^0}{RT^0}\right)^{n-1} \exp\left(-\frac{E_a}{\tilde{R}T}\right) \tag{20}$$

Consequently, for reaction orders different from 1, the dominant balance no longer holds. This effect of the pressure will be investigated in the following sections by varying the pressure and studying the effect of the effective reaction order.

2.3 Effect of Equivalence Ratio

Changes in the equivalence ratio change the energy content of a mixture as well as the chemical reaction rate, in particular when the mixture changes from fuel-lean to fuel-rich. In our one-step model we capture the later by accounting for changes in the energy content through q_c, and the former by changing the activation energy, E_a. The calculation of both parameters is detailed in the next section.

3 Calculation of Model Parameters

In our thermal ignition model a number of parameters are fixed by the physical system used in the experimental study [2]. These parameters are highlighted in the second section of Table 1. The other parameters, shown in the third section of Table 1, are determined with the use of a detailed chemical model and the available experimental data.

Table 1: Nomenclature and Model Parameters

Parameter	Value	Units	Description
T		K	temperature
p		atm	pressure
ρ		kg m^{-3}	density
α		K s^{-1}	wall temperature heating rate
X			mole fraction
Y			mass fraction
λ			progress variable
W		kg/kmol	mixture molecular weight
V	4.273E-4	m^3	volume
S	0.05	m^2	surface area
h	15	J s^{-1} m^{-2} K^{-1}	heat transfer coefficient
c_v	980	J kg^{-1} K^{-1}	specific heat at constant volume
$\tilde{R}$	8314.47	J kmol^{-1} K^{-1}	universal gas constant
q_c		J kg^{-1}	chemical energy content
E_a		J kmol^{-1}	activation energy
A		s^{-1}	pre-exponential
Z		s^{-1}	lumped pre-exponential
$(\bullet)_w$			value at the wall
$(\bullet)_i$			value for species i
$(\bullet)^0$			initial value
$\dot{(\bullet)}$		s^{-1}	rate of change of $\bullet$

3.1 Heat transfers

The heat transfer coefficient is determined from the experimental observation that the transition from a slow reaction to a fast reaction occurs as the heating rate is increased from 5 K/min to 10 K/min. This transition occurs for a slightly fuel-rich mixture ($\phi = 1.2$), at atmospheric pressure for a heat transfer coefficient of 15 W/m^2-K [2]. While the current value is consistent with free convection of gases [9], it is of interest for further studies to study its variation with vessel geometry and material.

3.2 Thermo-chemical parameters

In order to include realistic thermodynamic and chemical parameters in the one-step reaction model, we performed a number of 0-D calculations with the detailed reaction model of Ramirez et al. [6] which we previously used to perform the detailed simulation study. It includes 420 chemical

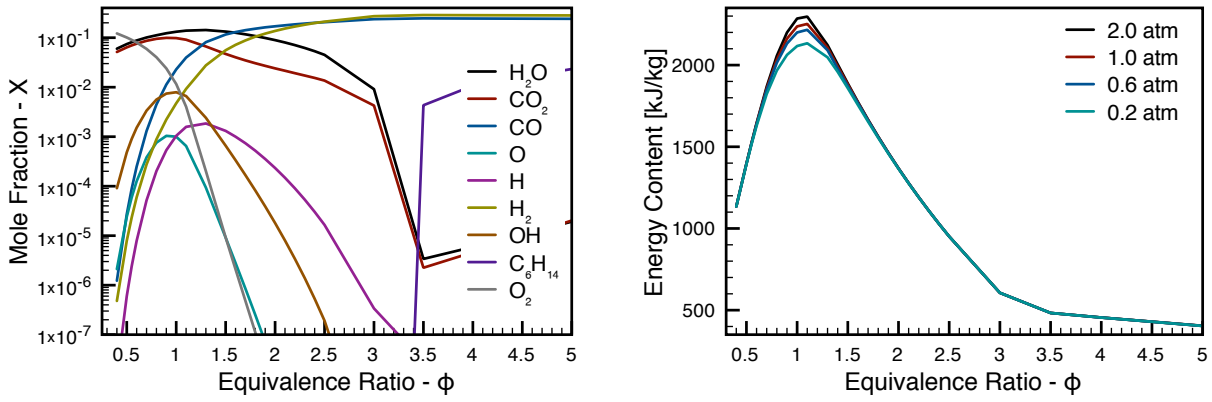

(a) Composition (b) Energy content

Figure 1: Evolution of the equilibrium composition (a) and of the energy content per unit of mass (b) as a function of equivalence ratio. Conditions: $T^0 = 298$ K and $p^0 = 1$ atm.

species and 1834 reactions.

3.2.1 Energy content

The first parameter that is calculated from the detailed mechanism is the energy content per unit mass, q_c. To calculate the energy content changes as a function of mixture composition and initial pressure, we consider the following global chemical reaction:

$$aC_6H_{14}+bO_2+cN_2 \rightleftharpoons dC_6H_{14}+eO_2+fN_2+gCO_2+hH_2O+iCO+jH_2+lH+mO+rOH \quad (21)$$

Coefficients a, b, and c are defined from the equivalence ratio taken into account while remaining coefficients are obtained from constant volume explosion computations. The energy content of the mixture corresponds to the standard enthalpy of reaction at 298 K per unit of mass.

Calculations were performed for $\phi = 0.4 - 5$, $T^0 = 298$ K and $p^0 = 0.2 - 2.0$ atm. Figure 1 (a) shows the evolution of the equilibrium composition as a function of equivalence ratio for an initial pressure of 1.0 atm. As expected, lean mixtures contain significant amounts of non-reacted oxygen while rich mixtures exhibit large amounts of CO and H_2. Figure 1 (b) displays the evolution of the enthalpy per unit of mass as function of equivalence ratio at various pressures showing only a small dependence on pressure for near stoichiometric mixtures. The shape of this curve is consistent with the shape of the evolution of the burning speed with equivalence ratio for hydrocarbon-based mixtures [3].

For each one-step simulation, the energy content is determined as a function of pressure and equivalence ratio from the pre-calculated dataset represented in Figure 1 (b) and linearly interpolated between data points.

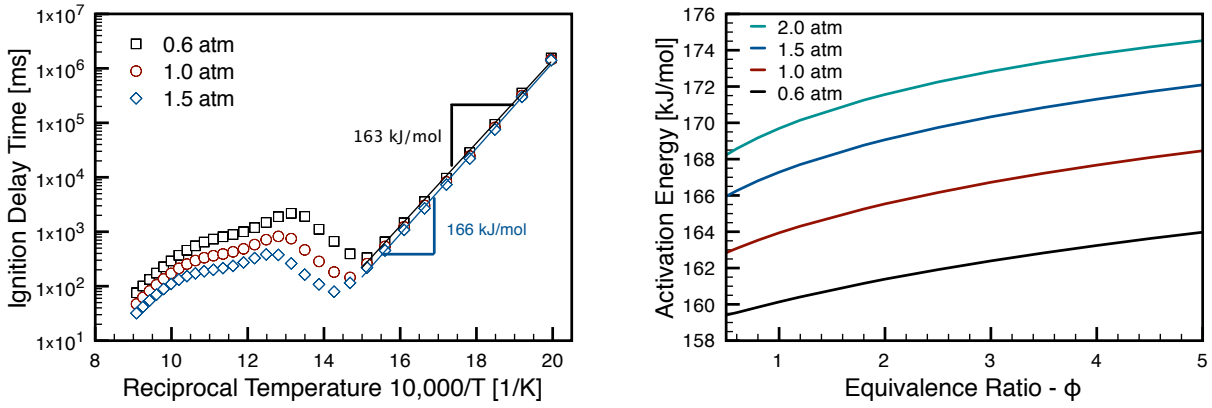

a) Ignition delay-time b) Activation energy

Figure 2: Evolution of the ignition delay-time a) and of the activation energy as a function of temperature and equivalence ratio, respectively. Conditions: $\phi = 0.5-5$; $T^0 = 500-1100$ K; $p^0 = 0.6-2.0$ atm.

3.2.2 Reaction Rate

The second parameter that is determined by use of the detailed mechanism is the activation energy, E_a. To obtain the activation energy as a function of pressure and equivalence ratio, we performed a series of ignition delay-time calculations assuming a constant volume reaction. The ignition delay-time is defined as the time to maximum pressure-gradient. Computations were performed over a period of 2000 s for $\phi = 0.4 - 5$, $p^0 = 0.2 - 2.0$ atm; and $T_0 = 500 - 1100$ K.

Figure 2 (a) shows the evolution of the ignition delay-time as a function of reciprocal temperature for the stoichiometric mixture and varying initial pressures. The different regimes of hydrocarbon oxidation are clearly seen: (i) the low-temperature oxidation; (ii) the negative temperature coefficient region; and (iii) the high-temperature regime. To obtain the activation energy in the low-temperature regime, we fitted the delay-time data for temperature between 500 and 650 K, as illustrated in Figure 2 (a).

Figure 2 (b) presents the evolution of the activation energy with equivalence ratio for different initial pressures. We observe that the activation energy exhibits both equivalence ratio and pressure dependencies.

Similar to the treatment of the energy content, for each one-step simulation, the activation energy is determined as a function of pressure and equivalence ratio from the pre-calculated dataset and linearly interpolated between data points.

The pre-exponential factor, Z, was calibrated so that the one-step model reproduces the transition from slow reaction to ignition observed in the detailed simulations at 1 atm for a stoichiometric mixture as the heating rate is increased from 10.75 K/min to 10.80 K/min. This transition behavior is shown in the one-step results for a stoichiometric mixture at atmospheric pressure in Figure 3. Figure 3 (a) shows the very slight temperature increase above the heating rate for the slow reaction case as well as the large temperature increase for the ignition case. Similarly, the reaction progress variable shows a steep increase in the reaction rate at the point of ignition in Figure 3 (b).

In the next section, results are shown for two different effect reaction orders, $n = 1$, and 2. For each of these effective reaction orders the pre-exponential is individually fit to $Z = 2.0 \times 10^{15}$ and 1.6×10^{15}, respectively. This approach is consistent with other one-step models [5, 8].

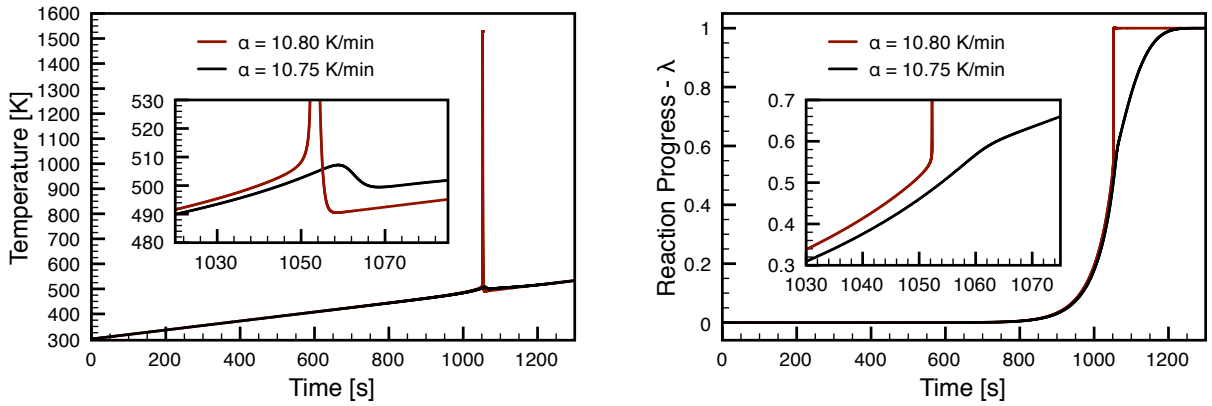

Figure 3: Simulation results for $n = 1$, $p^0 = 1$ atm, and $\phi = 1.0$ showing the (a) temperature evolution and (b) progress variable evolution for a slow reaction and an ignition case with a small heating rate increase of 0.05 K/min.

4 Results and Discussion

Solutions to the one-step thermal ignition model are obtained for a pressure range of $p^0 = 0.2-2.0$ atm over flammability range $\phi = 0.55-3.5$ at standard temperature and pressure [10]. The heating rate is varied from $\alpha = 1$ K/min to 30 K/min to investigate the transition behavior

An ignition case is distinguished from a slow reaction case by the temperature overshoot, ΔT, above the prescribed by the heating rate. The transition is marked by a threshold temperature overshoot of 50 K. Figure 4 shows this transition in ΔT as a function of heating rate at 1 atm for a stoichiometric mixture.

$$\Delta T = \max(T(t) - \alpha\, t - T_w^0) \tag{22}$$

With the distinction between slow reaction and ignition cases made clear, we can now show the behavior of a large number of initial conditions by identifying them only as ignitions and slow reactions. Figure 5 (a) shows the results for simulations with an initial pressure of 1 atm. We observe that for the range of heating rates investigated, mixtures between $\phi = 0.55$ and 2.5 transition from slow reactions to ignition as the heating rate is increased. The required transition heating rate is, however, not a constant, but depends on the equivalence ratio. This dependence on the composition is a result of the energy content of the mixture and the activation energy, which are both modeled as functions of pressure and equivalence ratio.

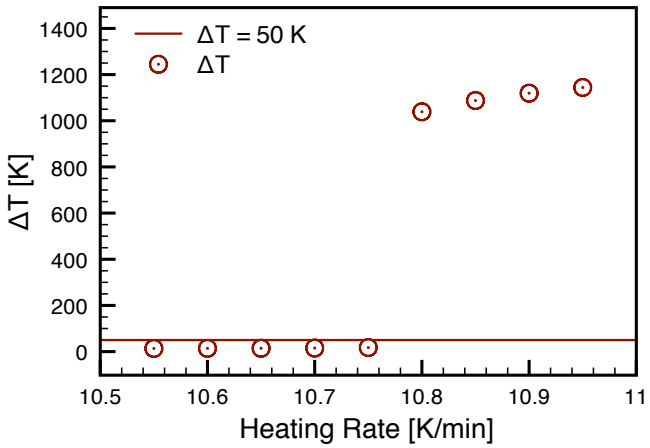

Figure 4: Temperature overshoot, ΔT, as a function of the heating rate for $n = 1$, $p^0 = 1$ atm, and $\phi = 1.0$ showing the transition from slow reaction to ignition with the threshold of $\Delta T = 50$ K.

The influence of mixture composition on energy content and activation energy can be partially investigated by fixing the activation energy and recalculating the ignition map as a function of equivalence ratio. In Figure 5 (b) the activation energy is fixed at the value obtained from the stoichiometric mixture; we observe that only a few cases exhibit a change in behavior. This suggests that the major contribution to the shape of the transition curve is due to the changes in the energy content with equivalence ratio. Note that the transition curve itself is plotted by fitting a sixth order polynomial fit to points between the ignition and slow reaction results.

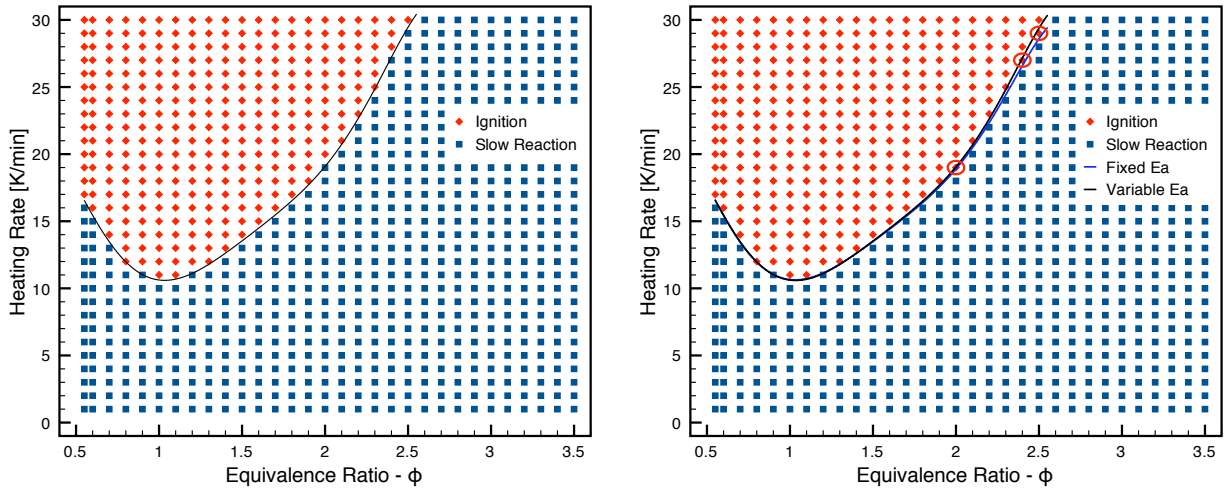

Figure 5: Ignition and slow reaction map for $n = 1$, $p^0 = 1$ atm, and $\phi = 1.0$ using (a) variable activation energy, $Ea(\phi)$ and (b) constant activation energy $Ea_{\phi=1} = 164$ kJ/mol. Cases that switch to ignition from slow reaction when the activation energy is fixed are highlighted in (b).

The final step in the current study is to investigate the change in behavior as the initial pressure is varied. As previously discussed, the initial pressure is expected to have an effect on the transition behavior as it is present in the energy loss term even when the effective reaction order is 1. The transition map as a function of all three variables, pressure, heating rate, and equivalence ratio is shown in Figure 6 (a). Each line represents the transition curve above which the mixture ignites and below which the mixture undergoes a slow reaction. In the appendix to this paper, the individual results and curve fits to the transition are provided for each pressure in Figures 8 and 9. The results show a clear monotonic trend in which with increasing pressure the ignition regime widens away from near-stoichiometric mixtures. Additionally, the heating rate required at a fixed equivalence ratio decreases with increasing pressure.

The results shown in Figure 6 (a) agree with the argument of dominant balance between the chemical heat release and the heat loss described in Section 2.2. We can see that as the pressure increases the mass inside the vessel and thereby the total amount of energy contained increases. The heat loss rate, however, is fixed by the surface area, heat transfer coefficient and temperature difference between the gas and the wall.

Next we change the effective reaction order to 2 so that the pressure also affects the energy release rate and the reaction progress. The results given in Figure 6 (b) show that same monotonic trend is still observed, but the individual transition curves have shifted. Specifically, we can observe that transition has shifted out of the investigated range for an initial pressure of 0.4 atm and has shifted up for 0.5 atm.

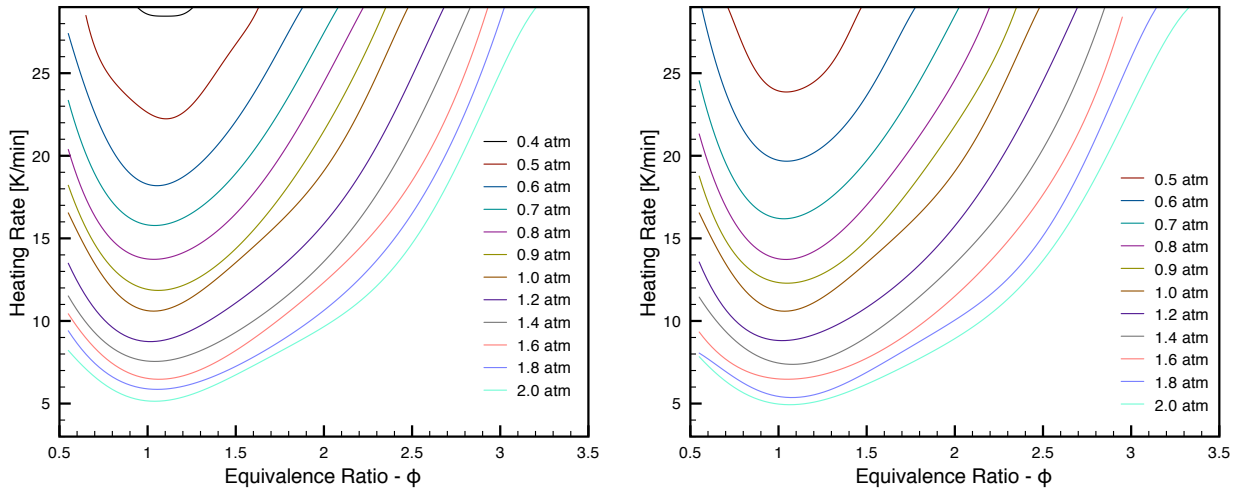

Figure 6: Contour plots of the transition curves for (a) $n = 1$ and (b) $n = 2$. Ignition occurs for initial conditions above the transition curve and a slow reaction occurs below.

Since the changes are somewhat difficult to discern in Figure 6 and the change is more pronounced at low pressure as compared to at high pressure, a more detailed view is required. Figure 7 shows the results at 0.5 and 2.0 atm for both $n = 1$ and $n = 2$. The results shown in blue squares are

cases for which both effective reaction order simulations result in a slow reaction. Similarly, all results shown in red diamonds are ignitions for both values. As we change the effective reaction order from 1 to 2 the transition curve shifts to higher heating rates as indicated by the arrows in Figure 7 (a). The initial conditions shown purple are ignitions for $n = 1$, but remain slow reactions when $n = 2$. Additionally, we can observe that the shift is smallest near stoichiometric conditions and increases away from $\phi = 1$ in both directions.

At higher pressures (Figure 7 (b)) the trend in n, however, is reversed. The arrows again indicate the direction of increasing effective reaction order. Shown green are the initial conditions which undergo an ignition for $n = 2$, but not $n = 1$. This illustrates that the transition curves pivot about a pressure in-between, which is $p^0 = 1$ atm. Simulation results confirm that for atmospheric pressure the results are the same for both effective reaction orders, which is expected but not guaranteed by the fact that the pre-exponential factor, Z, is calibrated to match the results of the detailed mechanism study for a stoichiometric mixture at atmospheric pressure.

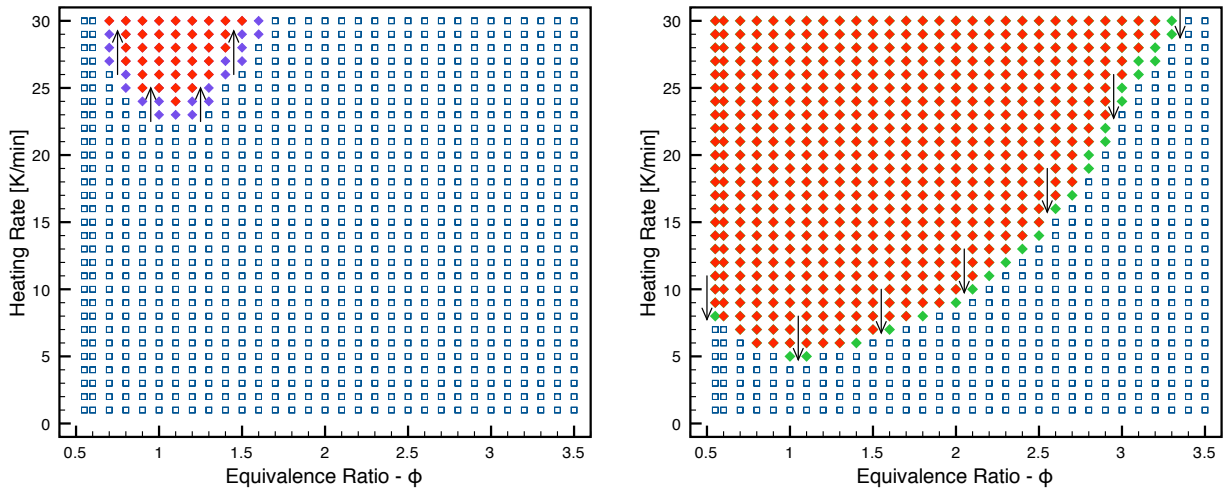

(a) 0.5 atm (b) 2.0 atm

Figure 7: (a) Shown in purple are the mixtures which ignite for $n = 1$, but not for $n = 2$ at $p^0 = 0.5$ atm, (b) shown in green are the mixtures which ignite for $n = 2$, but not $n = 1$ at $p^0 = 2.0$ atm. Arrows indicate the direction of increasing the effective reaction order, n, from 1 to 2.

5 Conclusions

The current study shows that the transition behavior of a homogeneous mixture undergoing ramp heating can be modeled with a one-step model for varying heating rates, mixture composition, and initial pressure. The transition from slow reaction to ignition is a function of all three variables showing that ignition will occur with increasing heating rate over a widening range of equivalence ratios as the initial pressure is increased. Future work will focus on investigating the effect of the wall material, by varying the heat transfer coefficient, h, and of the overall reactor geometry, by varying the surface to volume ratio, S/V.

6 Appendix

The following plots are the raw results for the simulations at n = 1.

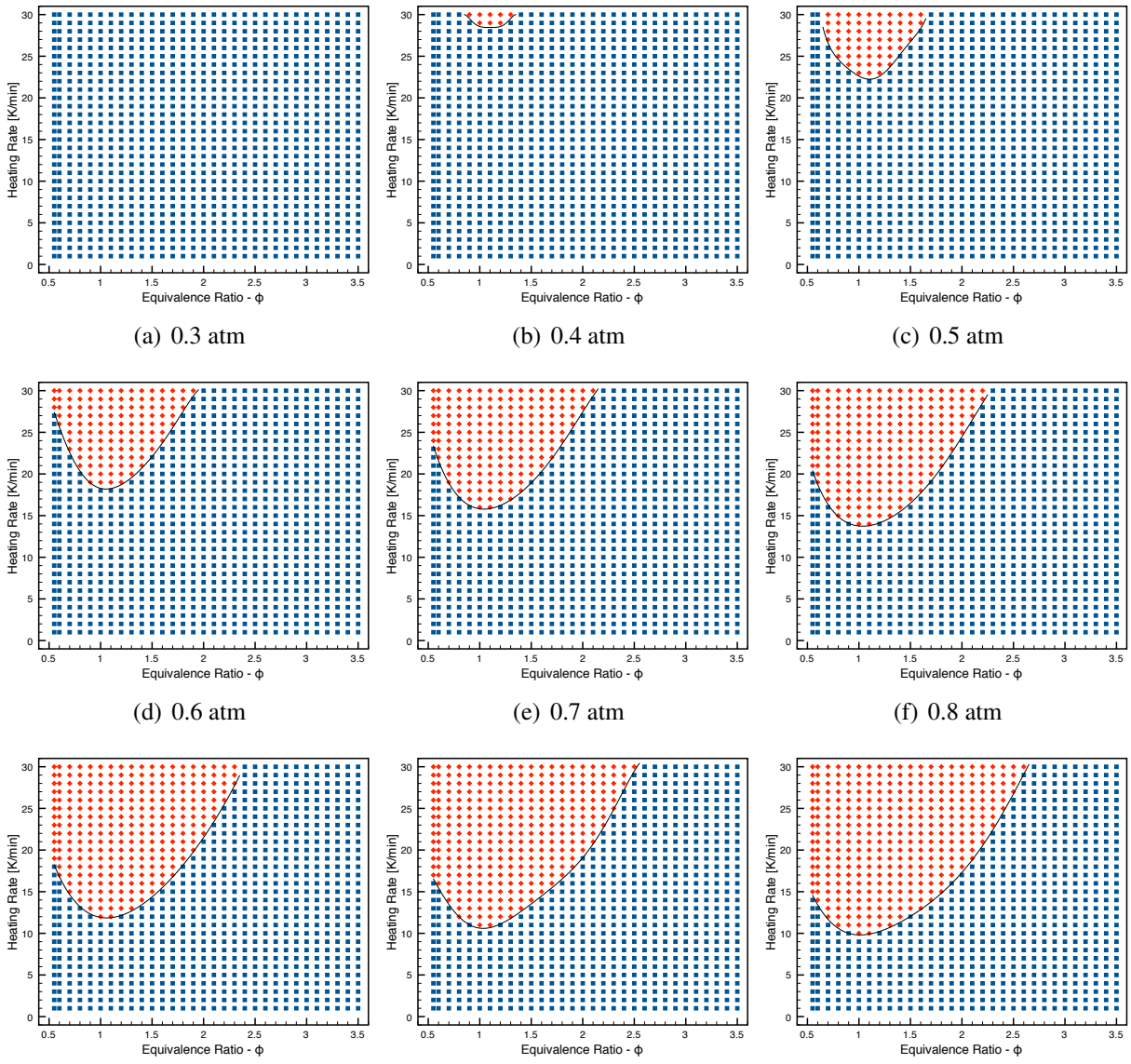

(a) 0.3 atm (b) 0.4 atm (c) 0.5 atm

(d) 0.6 atm (e) 0.7 atm (f) 0.8 atm

(g) 0.9 atm (h) 1.0 atm (i) 1.1 atm

Figure 8: Map of initial conditions leading to ignition (red) or slow reactions as a function of equivalence ratio and heating rate at various initial pressure $n = 1$

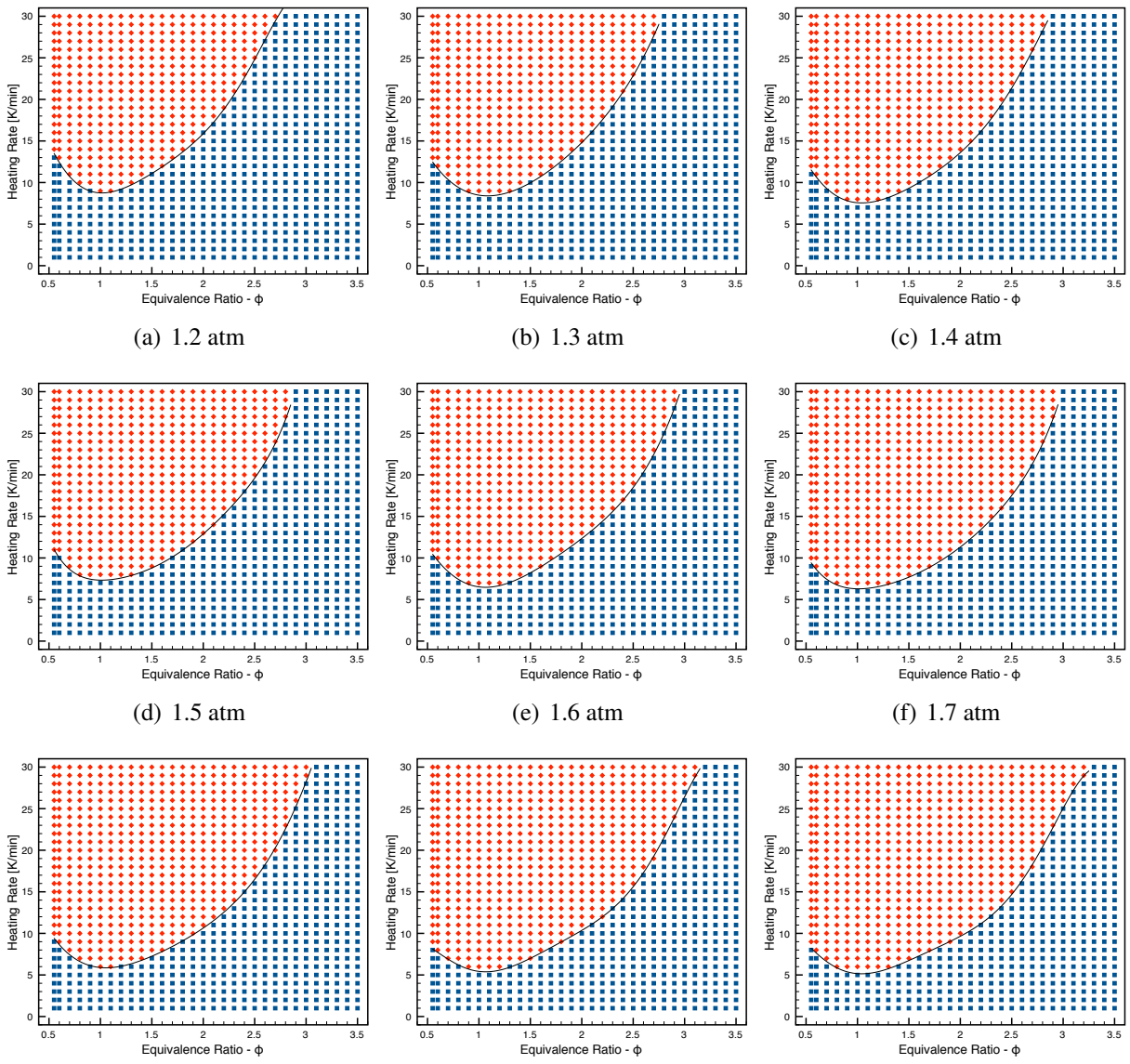

(a) 1.2 atm (b) 1.3 atm (c) 1.4 atm

(d) 1.5 atm (e) 1.6 atm (f) 1.7 atm

(g) 1.8 atm (h) 1.9 atm (i) 2.0 atm

Figure 9: Map of initial conditions leading to ignition (red) or slow reactions as a function of equivalence ratio and heating rate at various initial pressure $n = 1$

References

[1] S. P. M. Bane, J. L. Ziegler, and J. E. Shepherd. Development of one-step chemistry models for flame and ignition simulation. *GALCIT Report GALTCITFM:2010.002*, 2010.

[2] P. A. Boettcher, R. Mével, V. Thomas, and J. E. Shepherd. The effect of heating rates on low temperature hexane air combustion. *Fuel*, 96:392–403, 2012.

[3] S. Coronel, Mevel R., P. Vervish-Kljakic, P. A. Boettcher, V. Thomas, N. Chaumeix, N. Darabiha, and J. E. Shepherd. Laminar burning speed of n-hexane-air mixtures. *Proceedings of the 8th Joint US Sections Meeting of the Combustion Institute, 2013*, 2013.

[4] I. Glassman. *Combustion*. Academic Press, San Diego, 4th edition, 2008.

[5] V. Guilly, B. Khasainov, H. Presles, and D. Desbordes. Simulation numérique des détonations à double structure cellulaire. *Comptes Rendus Mecanique*, 334(11):679–685, 2006.

[6] H. P. Ramirez, K. Hadj-Ali, P. Dievart, G. Dayma, C. Togbe, G. Moreac, and P. Dagaut. Oxidation of commercial and surrogate bio-diesel fuels (B30) in a jet-stirred reactor at elevated pressure: Experimental and modeling kinetic study. *Proceedings of the Combustion Institute*, 33:375–382, 2011.

[7] N. N. Semenov. Thermal theory of combustion and explosion. *Progress of Physical Science*, 23, 1940. English Version: Technical Memorandums - National Committee for Aeronautics No.-1024 (NACA 1024).

[8] C. K. Westbrook and F. L. Dryer. Simplified reaction mechanisms for the oxidation of hydrocarbon fuels in flames. *Combustion science and technology*, 27(1-2):31–43, 1981.

[9] F. M. White. *Heat Transfer*. Addison-Wesley, Boston, MA, 1984.

[10] M. G. Zabetakis. Flammability characteristics of combustible gases and vapors. Technical report, Bureau of Mines, 1965. Bulletin 627.